Available online at http://scik.org
Commun. Math. Biol. Neurosci. 2019, 2019:14
https://doi.org/10.28919/cmbn/3606
ISSN: 2052-2541

THERMOGRAPHIC PATTERN'S IN WOMEN'S BREAST DUE TO UNIFORMLY PERFUSED TUMORS AND MENSTRUAL CYCLE

AKSHARA MAKRARIYA[1,*], NEERU ADLAKHA[2]

[1]School of Advanced Sciences-Mathematics, VIT Bhopal University, (M.P.), India

[2]Department of Mathematics and Humanities, SVNIT, Surat, Gujrat, India

Abstract. The investigators in the past studied thermographic patterns due to malignant tumors in the breast without taking into account the benign changes taking place in the breast during her life time. The thermography being non-destructive in nature is preferable over other techniques for detection of breast cancer. But it suffers from the issues of specificity and sensitivity. These issues may be due to various benign changes in the breast in response to physiological processes taking place in womens body. In this paper a model is proposed to study thermographic patterns in womens breast due to uniformly perfused tumor in presence and absence of benign changes taking place due to menstrual cycle. The finite element technique is employed to simulate the model. The numerical results have been used to study the effect of follicular and luteal phases of menstrual cycle on thermographic patterns in womens breast with and without tumor. The results obtained from such models can be useful for improving the specificity and sensitivity of detection of tumors and other malignant and benign disorders in womens breast by thermography.

Keywords: thermal conductivity; triangular ring element; uniformly perfused tumor; menstrual cycle.

2010 AMS Subject Classification: 92C35, 65L60.

*Corresponding author

E-mail address: aksharahul@gmail.com.

Received December 10, 2017

1. Introduction

Thermography is prefered over mammography and ultra sound because it is non invasive radiation and pain free imaging approach and it is non destructive in nature. Thermography uses infrared detectors to detect heat and increased vascularity that may be related to angiogenesis. It can detect physiological changes years prior to any other screening method. It is also very sensitive to fast growing aggressive tumors. Thermography can work as earlist warning system with breast tissues and physiological changes. Its average senstivity and specificity is 90% each [42].

Premenstrual breast swelling and tenderness, or cyclical mastalgia, is a common concern among women. The symptom is part of a group of symptoms called premenstrual syndrome, or PMS. Premenstrual breast swelling and tenderness can also be a sign of fibrocystic breast disease. Fibrocystic breast disease is a term used to describe painful, lumpy breasts prior to the menstrual period. Women with this condition often notice large, benign (noncancerous) lumps in their breasts prior to their monthly periods. Fluctuating hormone levels account for most episodes of premenstrual breast swelling and tenderness. The hormones rise and fall during a normal menstrual cycle. The exact timing of the hormonal changes varies for each woman. Estragon causes the breast ducts to enlarge. Progesterone production causes the milk glands to swell. Both of these events can cause the breasts to feel sore. Estragon and progesterone both increase during the second half of the cycle days 14 to 28 in a “typical” 28-day cycle [41]. Estragon peaks in the middle of the cycle, while progesterone levels rise during the week before menstruation. The hormonal activity in the breast will affect thermographic imaging to some degree [42]. Hormonal changes occur during menstrual cycle, physical stress, mental stress, physiological stress and with the increasing age, change in climatic condition and eating habits. Thus, the benign changes in womens breast during menstrual cycle can affect the thermographic patterns in womens breast. This may lead to false positive and false negative test for women with breast tumour during various phases of menstrual cycle. The study of thermographic patterns in womens breast involving malignant tumour during various phases of menstrual cycle will give us better insights of thermographic relationship with malignant and benign changes in womens

breast which in turn will be useful for having better insights of thermographic specificity and sensitivity due to these benign and malignant changes.

Patterson [26] performed the experimental investigations to study temperature distribution in the human peripheral region. The theoretical investigations are also reported in the literature for study of temperature distribution in peripheral tissues of flat regions of human body like trunk [10, 11, 12, 13, 33, 34, 35], the cylindrical shaped human organs like limbs [1, 2, 4, 5, 6, 13, 36,37] and spherical shaped organs like human head [15, 16, 17,18, 19] and womans breast [19,22,24] under normal, physiological and environmental conditions. Also, theoretical studies on thermal effect of malignant tumors in various regions of human body like flat, cylindrical and spherical shaped organs [3, 20, 21, 23, 26, 27, 28, 29, 39, 40] are reported in the literature. Acharya , Saxena & Gurung [7,8] studied temperature distribution in dermal layers of male versus female subjects under normal, environmental and physiological conditions for one and two-dimensional cases. Acharya Saxena & Gurung [9] investigated this temperature distribution in peripheral regions of female subject during menstrual cycle.

From the literature survey, it is evident that very little attention is paid to study the thermal effect of tumor during menstrual cycle of women's breast. No investigation is reported for the study of effect of tumors on temperature in womens breast during various phases of the menstrual cycle. In this paper, a model is proposed to study the thermal changes in womens breast due to malignant and benign disorders like tumors and different phases of menstrual cycle. The mathematical model and method are presented in the next section.

2. Mathematical Models

For a two-dimensional steady state case, the partial differential equation for heat flow in spherical organs of human body is given by [32]:

$$\frac{1}{r^2}\frac{\partial}{\partial r}\left(Kr^2\frac{\partial T}{\partial r}\right)+\frac{1}{r^2\sin\theta}\frac{\partial}{\partial\theta}\left(K\sin\theta\frac{\partial T}{\partial\theta}\right)+m_b c_b\left(T_A-T\right)+\overline{S}=0 \tag{1}$$

Where K= thermal conductivity of tissue, m_b = blood mass flow rate, c_b = specific heat of blood, T_A = blood temperature, T = tissue temperature at position r measured from the center towards skin surface , $\overline{S}$ = rate of metabolic heat generation in tissue. We consider $T_A = T_b$ as the blood

flows in arteries from core at body core temperature $T_b = 37^{\circ}C$ .In order to incorporate the metabolic heat generation in normal and malignant tissues, the term $\overline{S}$ is expressed as

$$\overline{S} = S + W \tag{2}$$

Here S represents controlled metabolic heat generation in normal tissues and W represents uncontrolled rates of metabolic heat generation in malignant tissues. The terms S and W will depend on position. In the regions of normal tissues W=0 while in malignant tissues W dominates over S and therefore S=0 [20].

The female breast is assumed to be hemispherical in shape. Also, the physiological structure is assumed to be symmetric along angular directions involving uniformly perfused tumor. The SST (Skin and Subcutaneous tissues) region of the breast is divided into the eleven layers, namely epidermis as one layer, dermis as nine layers and subcutaneous tissues as one layer. Here the properties are most variable in the dermis layers. Also, the elliptical shaped tumor is assumed to be present in the dermis. Therefore, dermis is divided in to nine layers to incorporate the shape of tumor. This shape is assumed in order to study the relationship between temperature profiles and the shape of the tumor. Considering elliptical shaped tumor gives us the flexibility to assign the different values to major and minor radius to match it with the different elliptical and spherical shapes of the tumor [20]. This can be done very easily in our model by giving appropriate data input in our program regarding radial and angular coordinates. Further the finer mesh in dermis gives us flexibility to assign independent values to the parameters in each element to incorporate variations in the properties of this layer.

The outer surface of the hemispherical region is exposed to the environment and heat loss at this surface takes place mainly due to conduction, convection, radiation, and evaporation [33]. Hence the boundary condition imposed at the outer surface is given by:

$$-K\frac{\partial T}{\partial r} = h(T - T_a) + LE \quad at \quad r = r_n \ , \quad \theta \in (0, \pi) \tag{3}$$

Where h is the heat transfer coefficient, Ta is the atmospheric temperature, L and E are, latent heat and rate of sweat evaporation, respectively. r_n is the radius of the outer surface of the breast.

The lower circle of the hemispherical region rests on the trunk of the human body. This region has angular coordinates $\varphi = 0$ to 2π. The core region of the breast at the base is near the trunk core and is maintained at T=T_b. The angular coordinate φ for semi-circle representing hemispherical surface bulging outwards from trunk lies between $\varphi = 0$ to $\varphi = \pi$. The points with $\varphi = \pi/2$ represent the extreme part of the breast core. This is also maintained at body core temperature for moderate and high atmospheric temperatures. But at lower atmospheric temperatures, the extreme part of the breast core will be at a lower temperature than that at the base of hemisphere [22]. Thus, two sets of boundary conditions at the core of breast are considered as given below:

2.1 Case I:

At moderate and higher atmospheric temperatures, the inner boundary of human breast is maintained at a uniform core temperature . Thus,

$$T(r,\theta) = T_b \quad at \quad r = r_0 \tag{4}$$

Where r_0 is the radius of core of the breast .

2.2 Case II:

At low atmospheric temperatures, the core temperature of woma's breast is variable along angular direction θ. This is because the warm blood flows in arteries at T_b from the core of the trunk to the core of woman's breast and the same blood reaching extreme (peripheral) parts of the breast by capillaries cools down and returns back from extremities of the breast through veins at lower temperature than the body core temperature [24]. Hence the following boundary condition is imposed

$$T(r,\theta) = F(\theta) \quad at \quad r = r_0 \tag{5}$$

Where $F(\theta) = g_1 + g_2\theta + g_3\theta^2$ and

$$\begin{aligned} T(r_0,\theta) &= \alpha \quad at \quad \theta = 0 \\ T(r_0,\theta) &= \beta \quad at \quad \theta = \pi/2 \\ T(r_0,\theta) &= \gamma \quad at \quad \theta = \pi \end{aligned} \tag{6}$$

Here α , and γ are the temperatures of the portion of core of the breast near the trunk and therefore taken to be equal to the body core temperature T_b . Here β is the temperature of the position of extreme part of the breast core ($\theta = \pi/2$) at a radial distance r_0 from the trunk and is generally lower than α , and γ at low atmospheric temperature. The values of the constants g_1, g_2 and g_3 are determined by using conditions (6).

Equation (1) along with the boundary conditions (3) and (4) in the variational form is written as given below:

(7)
$$I^{(e)} = \frac{1}{2}\iint_{\Omega}\left[K^{(e)}r^2\left(\frac{\partial T^{(e)}}{\partial r}\right)^2 + K^{(e)}\left(\frac{\partial T^{(e)}}{\partial \theta}\right)^2 + \left\{M^{(e)}\left(T_A^e - T^{(e)}\right)^2 - \left(S^{(e)} + W^{(e)}\right)\right\}r^2 dr d\theta\right]$$
$$+\frac{\lambda^{(e)}}{2}\int_{\Omega_1}\left\{h\left(T^{(e)} - T_a\right)^2 + 2LET^{(e)}\right\}r^2 d\theta \quad for \quad e = 1(1)352$$

Where $\Omega(r,\theta)$ is the boundary of e^{th} element and Ω_1 is the boundary of outer surface $K^{(e)}, M^{(e)}$, $S^{(e)}, W^{(e)}, T_A^{(e)}$ and $T^{(e)}$ denote the values of K, M, S, W, T_A respectively in e^{th} element. $\lambda^{(e)}$=1 for elements along the surface and $\lambda^{(e)}$=0 for all elements which are not along the outer surface. The region is discretized into three hundred fifty-two triangular ring elements of different sizes in order to match the geometry of the region and incorporate the minute details of physiology such as structure and in homogeneity of the region [20]. As shown in Fig (1), dividing the region into a sufficient number of elements gives us flexibility in assigning the independent values to the physical and physiological parameters in each sub region. The blood flow and metabolic activity in a tumor is found to vary between 0 to 7 times of that in normal tissues [28]. Accordingly, the different values have been assigned to blood mass flow and metabolic heat generation in uniformly perfused tumors.

The following bilinear shape function for variation of temperature within each element has been taken as:

(8)
$$T^{(e)} = c_1^{(e)} + c_2^{(e)}r + c_3^{(e)}\theta$$

$c_1^{(e)}$, $c_2^{(e)}$, and $c_3^{(e)}$ are constants for the e^{th} element.

The element sizes are taken to be smaller in dermis and tumor. As the variations in the physical and physiological parameters are more in these sub regions. However, the properties

are almost uniform in sub dermal tissues and epidermis, hence elements of bigger size have been used to discretize these sub regions. As a particular case, the following values have been assigned to the parameters K, M, S and W for each element.

3. Values of parameters

3.1 Parameters for each element when N=352:

Sub dermal Tissues: (e=1 (22) 331 and 2 (22) 332)

$$K^{(e)} = K_1, M^{(e)} = M_1, S^{(e)} = S_1, W^{(e)} = 0$$

Dermis (Normal Tissues): (e=i(22) 330+i ; i = 3 (1) 18)

$$K^{(e)} = K_2, M^{(e)} = M_2, S^{(e)} = S_2, W^{(e)} = 0$$

Epidermis: (e=21 (22) 351 and e= 22 (22) 352)

$$K^{(e)} = K_3, M^{(e)} = M_3, S^{(e)} = S_3, W^{(e)} = 0$$

Tumor Region: (e= 120 to 125, 140 to 149, 161 to 172 ,183 to 194 , 206 to215, 230 to 235)

$$K^{(e)} = K, M^{(e)} = M_1, S^{(e)} = 0, W^{(e)} = \eta^{(e)} S_1$$

Here N is the number of elements

3.2 Parameters for each element when N=704:

Sub dermal Tissues: (e=1 (22) 683 and 2 (22) 684)

$$K^{(e)} = K_1, M^{(e)} = M_1, S^{(e)} = S_1, W^{(e)} = 0$$

Dermis (Normal Tissues): (e=i(22) 680+i ; i = 3 (1) 18)

$$K^{(e)} = K_2, M^{(e)} = M_2, S^{(e)} = S_2, W^{(e)} = 0$$

Epidermis: (e=21 (22) 703 and e= 22 (22) 704)

$$K^{(e)} = K_3, M^{(e)} = M_3, S^{(e)} = S_3, W^{(e)} = 0$$

Tumor Region: (e= 231 to 235, 250 to 259, 271 to 282, 293 to 304, 315 to326, 337 to 348, 359 to 370 , 381 to 392, 403 to 414 , 425 to 436, 448 to 457 and 472 to 477)

$$K^{(e)} = K, M^{(e)} = M_1, S^{(e)} = 0, W^{(e)} = \eta^{(e)} S_1$$

Using above values of parameter, the integral (7) is evaluated for each element and assembled to obtain.

$$I = \sum_{i=1}^{n} I \tag{9}$$

The integral I is minimized with respect to each nodal temperature T_i. i = 1, 2, 3,- - -, n. This leads to a system of linear algebraic equations given below;

$$[X]_{n\times n}\left[\overline{T_{n\times 1}}\right] = [Y]_{n\times 1} \tag{10}$$

Here, $\overline{T} = \begin{bmatrix} T_1 & T_2 & T_3 & - & - & - & - & T_n \end{bmatrix}^T$, Where T_n denotes the n^{th} nodal point temperature and n is the number of nodal points= 204.

The Gauss elimination method has been used to obtain the solution of system (10). A computer program in MATLAB 10.11 is developed to find numerical solution to the entire problem. The time taken for simulation is nearly 2 minutes on Core(TM) i7 CPU M 7580 @ 2.13 GHz processing speed and 8 GB memory.

4. Numerical Results

The numerical results are obtained using the values of the physical and physiological constant [28,29] given below:

K1= 0.060 cal/ cm-min-deg^0C, K2= 0.045 cal/ cm-min-deg^0C , K3=0.030 cal/ cm-min-deg^0C , K=0.0845 cal/ cm-min-deg^0C , Tb= 37^0C , h= 0.009 cal/cm^2-min-deg^0C , L=579 cal/gm. , The values of M, S, and E used in this study are given in Table 1: $M_2 = M_1/2, M_3 = 0, S_2 = S_1/2, S_3 = 0$.

The simulation was performed for N=352 elements initially. Then again, the simulation was performed by taking N=704 elements. We get a temperature of 36.4666 at node number 103 in women's breast during luteal phase of menstrual cycle with uniformly perfused tumor for model with N=352 elements and temperature 36.4676 at node number 199 in women's breast during

TABLE 1. Values of Parameters (Saxena, Bindra and Pardasani 1984, 1991, Acharya, Gurung & Saxena.2014)

Atmospheric tem.	M_{max}	S_max	E
15^oc	0.003	0.0357	0.0
23^oc	0.018	0.018	0.0, 0.24 x 10^{-3}, 0.48 x 10^{-3}
33^oc	0.315	0.018	0.0, 0.24 x 10^{-3}, 0.48 x 10^{-3}, 0.72 x 10^{-3}

Atmospheric tem.	m_b follicular	m_b luteal	$S_{follicular}$	S_{luteal}
15^oc	0.01538	0.02197	0.0665	0.0707
23^oc	0.09228	0.13182	0.03325	0.03535
33^oc	0.1538	0.2197	0.03325	0.03535

luteal phase of menstrual cycle with uniformly perfused tumor for model with N=704 elements. The error is [(36.4676 - 36.4666)/36.4676] *100 which works out to be 27.42 x 10^{-6}% only. For better clarity, we take the ratio to four decimal places (0.4666/0.4676) * 100=99.78% and call this the confidence level. A confidence level of 100 implies that a saturation point has been reached. In this paper, the simulation was performed by increasing the number of elements N= 1056, 1408, 1760, 2112. The saturation point was achieved for N=1760. In this work, we have used N=352 elements as the number of elements in our models as we can safely say that results are mesh insensitive at this number.

For a particular sample of peripheral tissue layers, r for the different layers is assigned the following values:

r_0=8cm; r_1=8.5 cm; r_2=8.54 cm; r_3=8.58 cm; r_4=8.62 cm; r_5=8.66 cm; r_6=8.7 cm; r_7=8.74cm; r_8=8.78 cm; r_9=8.82 cm; r_{10}=8.9 cm; r_{11}=9.1 cm

5. Discussion:

5.1 Case: I

Graphs have been plotted among T, r and θ for different values of atmospheric temperatures, E and η. Where η is parameter to represent ratio of metabolic activity in tumor and normal

tissues, which is found to vary between 1 to 7 times of that in normal tissues. Here for particular samples of tumor we take η=5.0 which implies that tumor has metabolic activity 5 times of that in normal tissues.

Figures 2 to 13 show the temperature distribution along r and θ in a women's breast. Figures 2 to 7 are for case -1 boundary condition and 8 to 13 are for case -II boundary condition, with and without tumor for normal case and during different phases of menstrual cycle. In these figures, the temperature reduces slowly from the breast core to the junction of sub dermal tissues and dermis and then the falls sharply as we move towards the outer surface. This is because the heat loss takes place from the outer surface to the environment. Also, the slope of the temperature profiles changes at the junctions of subdermal tissues and dermis, and dermis and epidermis. This is because of the different physiological properties of each layer. The maximum thermal disturbances are observed in and around the tumor region in the dermal part of the breast. Further, these thermal disturbances are higher during luteal and follicular phases of menstrual cycle as compared to those without menstrual cycle. In Figures 5, 6 and 7, η=0 represents absence of tumor. In Figures 5, 6 and 7, it is observed that gaps between curves are more in Fig 7 for luteal phase as compared to Fig 6 for follicular phase and Fig 5 for normal case i.e. without menstrual cycle. This implies that thermal effect in Fig 6 is more visible than that in Fig 5 and the thermal effect of tumor in Fig 7 is more visible as compared to that in Fig6. The results obtained here for the normal case are in agreement with biological facts and those obtained by earlier research workers [28,20].

5.2 Case: II

The temperature profiles for peripheral regions of the women's breast involving a tumor have been computed using the variable boundary condition and are shown in Figures (8), (10) and (12) for T_a = 15^{o}C, E=0 and η = 5.0 respectively. It can be observed that the temperature varies between 37 and 36^{0}C at r = 8 cm along the angular direction in the core of breast. This parabolic variation of temperature at the inner boundary is because of the variable boundary condition. Also, the effect of the parabolic variation of temperature at the inner boundary is observed on the temperature profiles in the region from inner core to the surface of the breast. We observe the change in the slope of the curves at the junctions of the normal tissues and tumor in all

these figures. The results obtained for normal case are in agreements with biophysical facts and results of earlier research workers [20,28].

Figures (9) (11) and (13) show the differences in temperature disturbances in women's breast due to presence of a tumor in absence of menstrual cycle and during different phases of menstrual cycle respectively. The peak values in Figures (9), (11) and (13) are 0.37^0C, 0.42^0C and 0.47^0C respectively. Thus, the thermal effect of tumor on surrounding tissues is higher in luteal phase as compared to that in follicular phase and this thermal effect of tumor in follicular phase is higher than that in case of absence of menstrual cycle. The peaks and ridges give us an idea about the location of different layers of uniformly perfused tumor in the woman's breast. The range of values of temperature difference because of the presence and absence of a tumor gives us an idea about the accuracy that is required by the equipment used to measure the temperatures in order to able detect to tumors. The maximum thermal disturbances are observed in and around the tumor region in the dermal part of the breast. Further, these thermal disturbances are higher during luteal and follicular phases of menstrual cycle as compared to normal days due to hormonal changes in women's breast during menstrual cycle. Thus, it is observed that the thermographic patterns in women's breast vary with the atmospheric temperature presence and absence of menstrual cycle and different types of tumors characterized by different rates of metabolic activity in tumors. In all it is observed that the nature of thermographic patterns due to malignant tumor in breast is similar in absence of menstrual cycle and in presence of follicular and luteal phases of menstrual cycle, but these thermographic patterns differ in magnitude for all the above three cases. This difference in magnitude of thermographic patterns can be useful to address the issues of specificity and sensitivity of thermal diagnosis of tumor.

6. Conclusion:

A finite element model is constructed and successfully employed to study the thermographic patterns in women's breast involving uniformly perfused tumor in absence and presence of menstrual cycle. On the basis of results, it is concluded that the follicular and luteal phases influence the thermographic patterns in women's breast in presence and absence of tumor. This influence of luteal and follicular phases will affect the diagnosis of tumor by thermography. The

effect of tumor on thermographic patterns in breast is more visible in luteal phase than that in follicular phase and this effect during follicular phase is more visible than that in normal case i.e. absence of menstrual cycle. Thus, it is concluded and recommended that the thermographic patterns in womans breast involving malignant tumor should be obtained by thermal imaging in absence of menstrual cycle and during both the follicular and luteal phases of menstrual to address the issues of sensitivity and specificity. The changes in magnitude of thermal patterns in all these three cases can be analysed for confirmation and rejection of the test in order to avoid the false negative and false positive results.

Acknowledgement:

Authors are grateful to Science and Engineering Research Board, Department of Science & Technology, New Delhi, India for providing assistance for this work under NPDF- Scheme. Also authors are thankful to Department of Biotechnology, New Delhi, India and M.P. council of Science and Technology, Bhopal, INDIA for providing Bioinformatics Infrastructure facility at MANIT, Bhopal, INDIA to carry out this work.

Author contributions statements:

N. Adlakha conceptualized the study. N. Adlakha & A. Makrariya developed the model and derived the equations. A. Makrariya performed computer simulation and complied the results. Both authors performed analysis the results and drafted the manuscript. Both authors have reviewed and approved the version of the manuscripts.

Conflict of Interests

The authors declare that there is no conflict of interests.

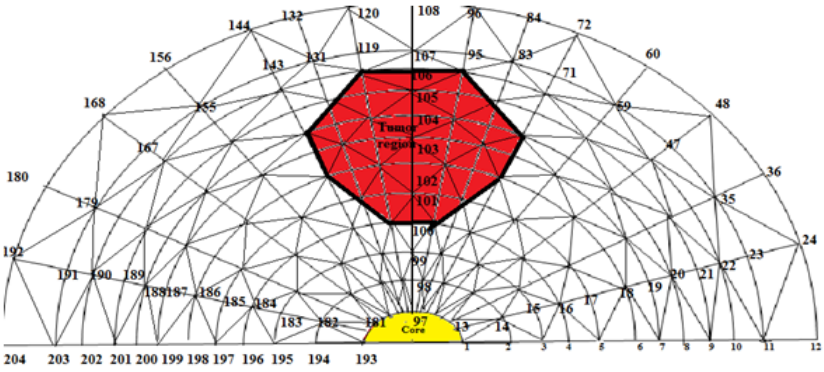

FIGURE 1. Discretization of region

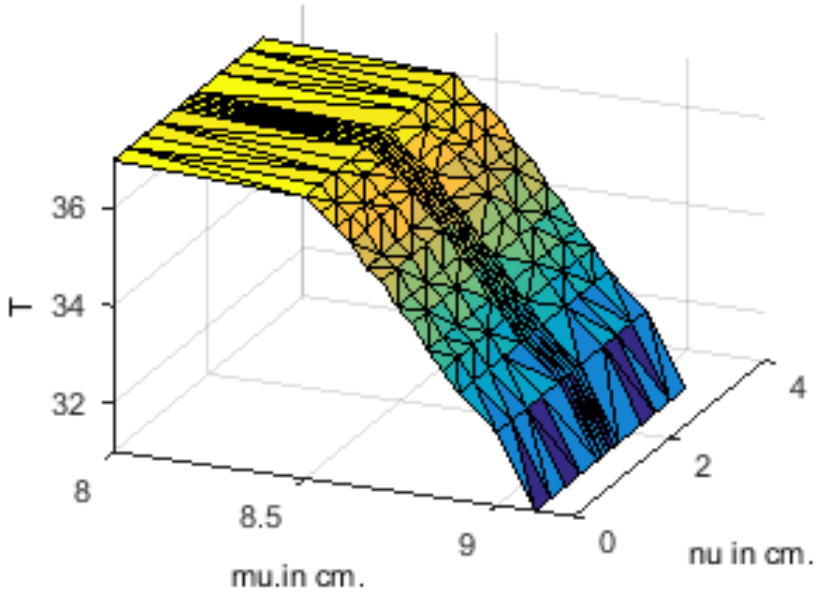

FIGURE 2. Temperature distribution along r and θ in normal condition womens breast without a tumor in absence of menstrual cycle for T_a=23^{0}C, E=0.24*10^{-3} Case-I boundary condition

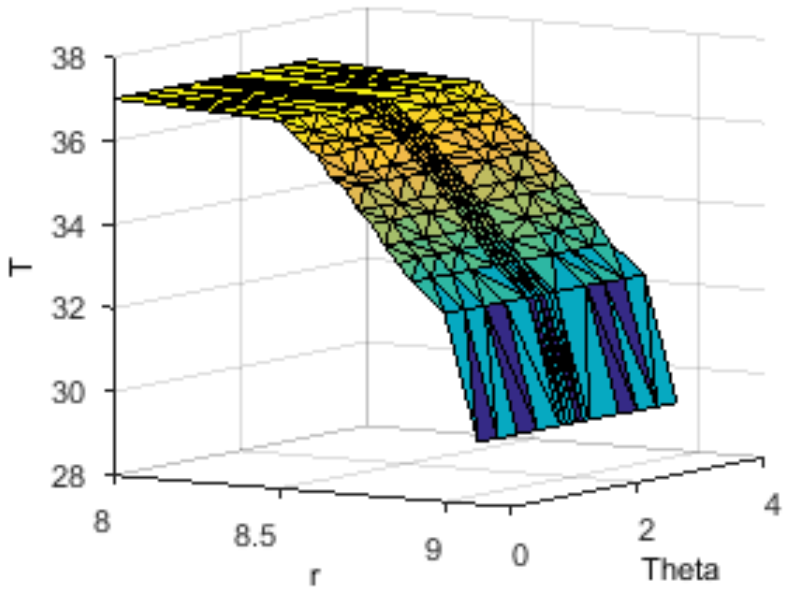

FIGURE 3. Temperature distribution along r and θ in womens breast without a tumor during follicular phase of menstrual cycle for T_a=23^{0}C, E=0.24*10^{-3} gm/cm^2min Case-I boundary condition.

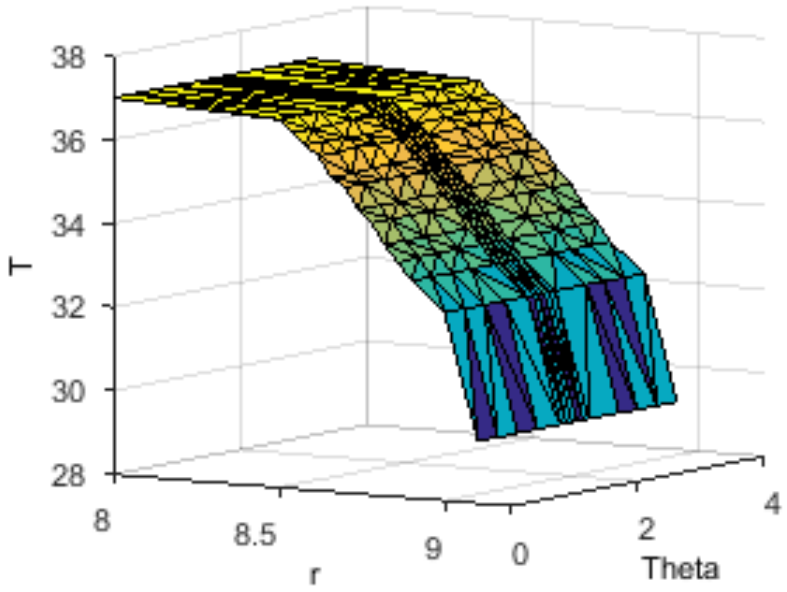

FIGURE 4. Temperature distribution along r and θ in womens breast without a tumor during luteal phase of menstrual cycle for T_a=23^{0}C, gm/cm^2min Case-I boundary condition.

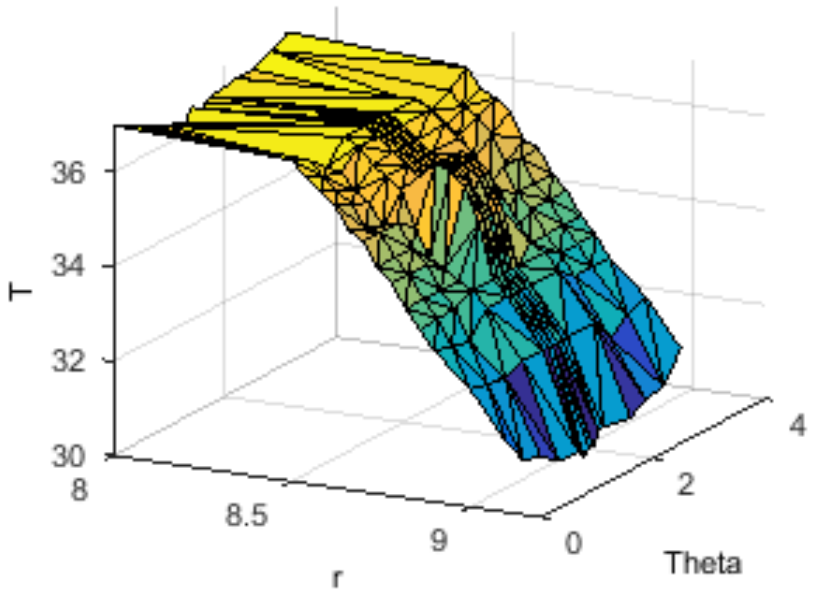

FIGURE 5. Temperature distribution along r and θ in normal condition womens breast with a tumor in absence of menstrual cycle for T_a=15^{0}C, E=0 gm/cm^2min, η=5.0 Case-II boundary condition,

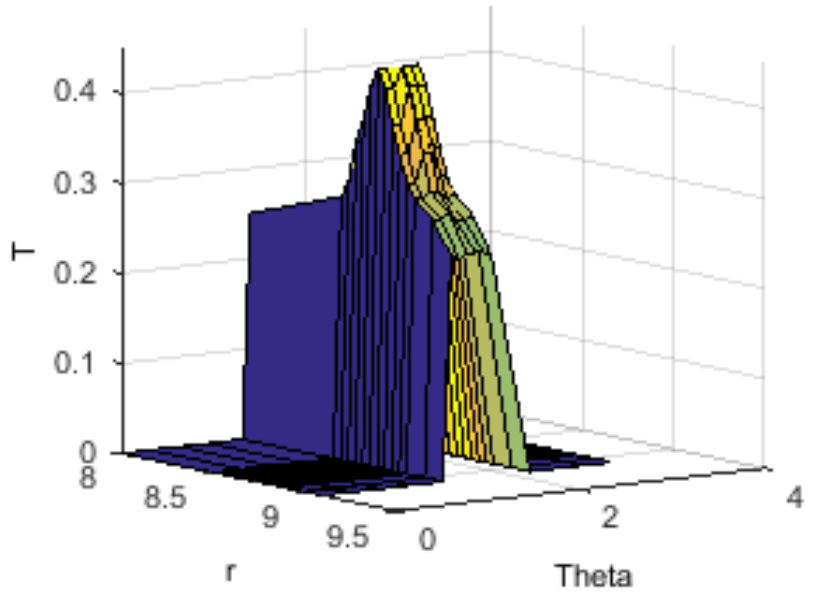

FIGURE 6. Distribution of temperature differences between womens breast with and without tumor in absence of menstrual cycle for T_a=15^{0}C, E=0 gm/cm^2min and η=5.0 Case-II boundary condition.

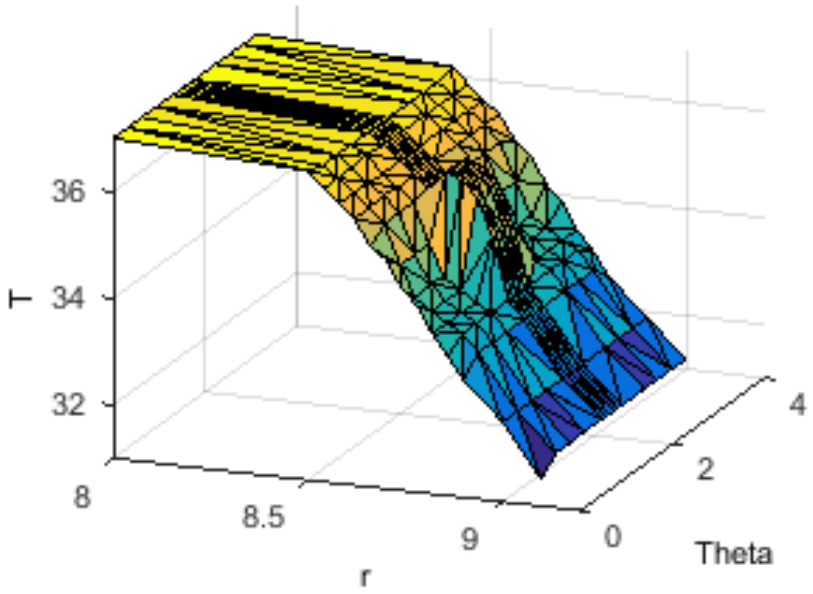

FIGURE 7. Temperature distribution along r and in womens breast with a tumor during follicular phase of menstrual cycle for T_a=150^{0}C, E=0 gm/cm^2min η=5.0 Case-II boundary condition.

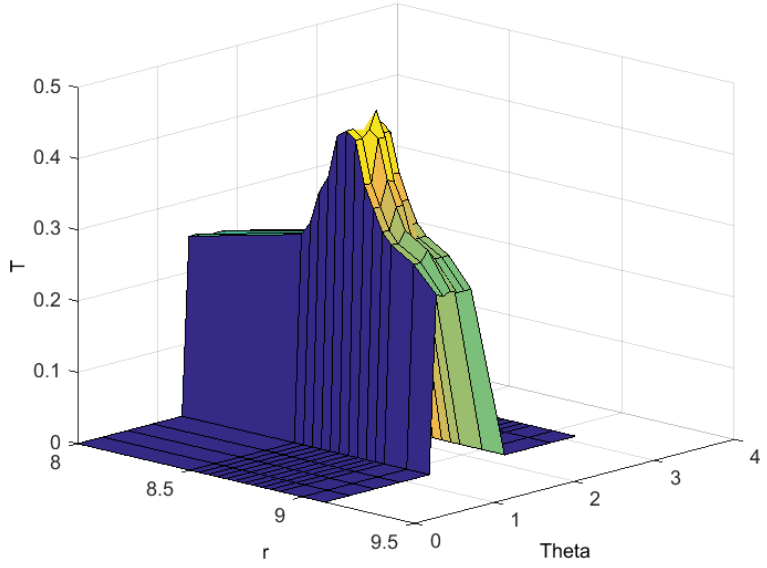

FIGURE 8. Distribution of temperature differences between womens breast with and without tumor during follicular phase of menstrual cycle for T_a=150^{0}C, E=0 gm/cm^2min and η=5.0 Case-II boundary condition

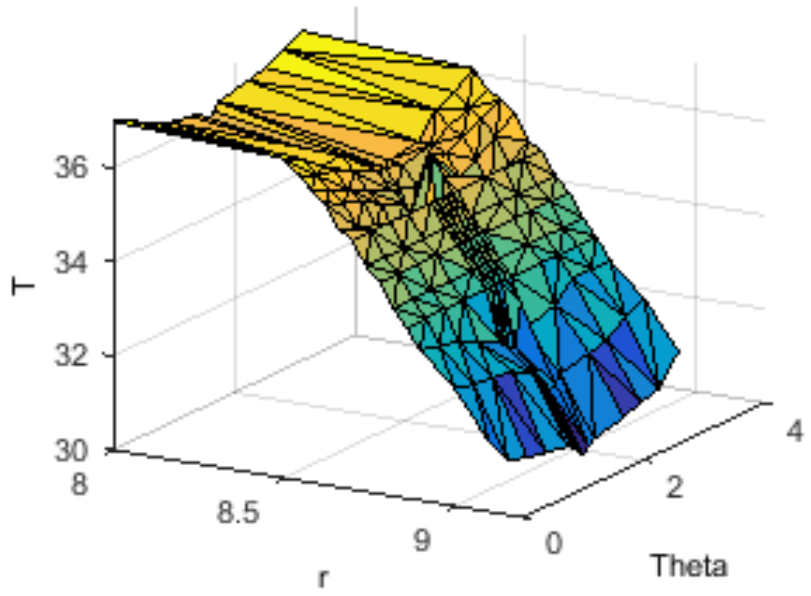

FIGURE 9. Temperature distribution along r and θ in womens breast with a tumor during luteal phase of menstrual cycle for T_a=150^{0}C, E=0 gm/cm^2min, η=5.0 Case-II boundary condition.

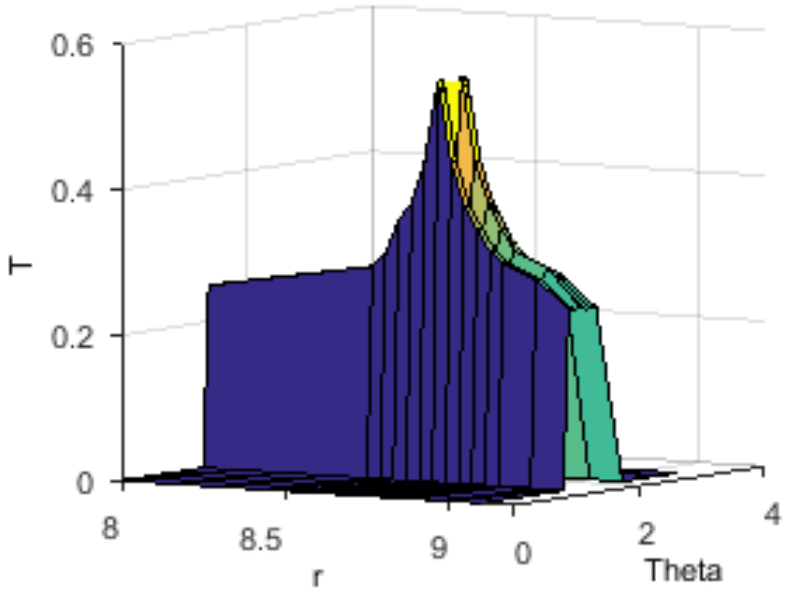

FIGURE 10. Distribution of temperature differences between womens breast with and without tumor during luteal phase of menstrual cycle for T_a=150^{0}C, E=0 gm/cm^2min and η=5.0. Case -II boundary condition.

REFERENCES

[1] M. Agrawal, N. Adlakha and K.R. Pardasani, Semi numerical Model to Study Temperature Distribution in Peripheral Layers of Elliptical and Tapered Shaped Human Limbs, J. Mech. Med. Biol. 10(1) (2010), 57-72.

[2] M. Agrawal, N. Adlakha and K.R. Pardasani, Three-Dimensional Finite Element Model to study heat flow in Dermal Region of elliptical and tapered shaped human limbs, Appl. Math. Comput. 217(8) (2010), 4129-4140.

[3] M. Agrawal, N. Adlakha, K.R. Pardasani, Finite Element Model to study Thermal Effect of Uniformly Perfused Tumor in Dermal layers of Elliptical Shaped Human Limbs. Int. J. Biomath. 4 (02) (2011), 241-254.

[4] M. Agrawal, K.R. Pardasani, N. Adlakha, , Finite element model to study the thermal effect of tumors in dermal regions of irregular tapered shaped human limbs, Int. J. Therm. Sci. 98 (2015), 287-295.

[5] M. Agrawal, K.R. Pardasani, N. Adlakha, Steady state temperature distribution in dermal regions of an irregular tapered shaped human limb with variable eccentricity, J. Therm. Biol. 44 (2014), 27-34.

[6] M. Agrawal, K.R. Pardasani, Finite element model to study temperature distribution in skin and deep tissues of human limbs, J. Therm. Biol. 62 (2016), 98-105.

[7] S. Acharya, D. B. Gurung and V. P. Saxena, Mathematical Modeling of Sex Related Differences in the Sensitivity of the Sweating Heat Responses to Change in Body Temperature, Br. J. Math. Computer Sci. 12(4)(2016), 1-11, Article ID 20068.

[8] S. Acharya, D. B. Gurung and V. P. Saxena, Human males and females body thermoregulation: Perfusion effect analysis, J. Therm. Biol. 45 (2014), 30-36.

[9] S. Acharya, D. B. Gurung and V. P. Saxena, Transient Temperature Distribution in Human Males and Females Body due to Variation in Perfusion Effect, Int. J. Appl. Math. 29 (2014), 1263-1270.

[10] K.N. Chao, W.J. Yang, Response of skin and tissue temperature in sauna and steam baths. Bio. Mech. Symp, ASME, AMD 1 (1975), 6971.

[11] T.E. Cooper, G.J. Trezek, A probe technique for determining the thermal conductivity of tissue. ASME J. Heat Transf. 94 (1972), 133140.

[12] D.B. Gurung, FEM approach to one dimensional unsteady temperature distribution in human dermal parts with quadratic shape function. J. Appl. Math. Inf. 27 (2009), 301-303.

[13] D.B. Gurung, Transient temperature distribution in human dermal part with protective layer at low atmospheric temperature. Int. J. Biomath. 3 (4) (2010), 439-451.

[14] P. Jas and K. R. Pardasani, Numerical simulation of the effect of polycythemia Vera ‘on heat flow in human dermal regions, Ind. J. Pure. Appl. Math. 31(12) (2000), 15951606.

[15] M. A. Khanday and V. P. Saxena, Finite element approach for the study of thermoregulation in human head exposed to cold environment. AIP Conf. Proc. 1146, 375 (2009).

[16] M.A. Khanday and F. Hussain, Explicit formula of finite difference method to estimate human peripheral tissue temperatures during exposure to severe cold stress, J. Therm. Bio. 48 (2014), 51-55.

[17] M.A. Khanday and K. Najar, Mathematical and numerical analysis of thermal distribution in cancerous tissues under the local heat therapy, Int. J. Biomath. 10 (07) (2017), Article ID 1750099.

[18] M. Mannu and R. M. Pidaparti, Breast tumor a simulation and parameters estimation using evolutionary algorithms, Model. Simul. Eng. 2008 (2008), Article ID 756436.

[19] A. Makrariya and N. Adlakha, Two-dimensional finite element model of temperature distribution in dermal tissues of extended spherical organs of a human body. Int. J. Biomath, 6 (2013), Article ID 1250065.

[20] A. Makrariya and N. Adlakha, Two - Dimensional Finite Element Model to Study Temperature Distribution in Peripheral Regions of Extended Spherical Human Organs Involving Uniformly Perfused Tumors, Int. J. Biomath. 8 (2015), Article ID 1550074 .

[21] A. Makrariya and N. Adlakha, Quantitative Study of Thermal Disturbances due to Non-Uniformly Perfused Tumors in Peripheral Regions of Womens breast, Cancer Inform. 16 (2017), 1-13 .

[22] M.M. Osman and E.M. Afify, Thermal modeling of the normal womans breast, J. Biomech. Eng. 106 (1984), 123-130.

[23] M.M. Osman and E.M. Afify, Thermal modeling of the malignant womans breast, J. Biomech. Eng. 110 (1988), 269- 276.

[24] M.M. Osman, Effect of arterio- venous heat exchange on breast temperature profile, J. Phys. III France, 4 (1994), 435-442.

[25] H. Pennes, Analysis of tissue and arterial blood temperature in the resting human forearm. J. Appl. Phys. 1 (1948), 93-122.

[26] A.M Patterson, Measurement of temperature profiles in human skin, South African J. Sci. 72 (1976), 78-79.

[27] K.R. Pardasani, and V.P. Saxena, Temperature distribution in skin and subcutaneous tissues with a uniformly perused tumor in the dermis. Proc. Natl. Acad. Sci. India Sec. A, 60 (1990), 11-20 .

[28] K.R.Pardasani and N. Adlakha, Exact solution to a heat flow problem in peripheral tissue layers with a solid tumor in the dermis, Ind. J. Pure. Appl. Math. 22 (1991), 679-687 .

[29] K.R. Pardasani and N. Adlakha, Coaxial circular sector elements to study two- dimensional heat distribution problem in dermal regions of human limbs, Math & Comp. Mod., 22 (1995), 127-140 .

[30] K.R. Pardasani and N. Adlakha, Two-dimensional Steady State Temperature Distribution in Annular Tissues of a human or animal body. Ind. J. Pure App. Math. 24 (1993), 721-728 .

[31] K.R.Pardasani and V.P.Saxena, exact solution to temperature Distribution problem in Annular Skin Layers. Bull. Calcutta Math. Soc. 81 (1989), 1-8.

[32] W Perl, Heat and matter distribution equation to include clearance by capillary blood flow, Ann. N.Y. Acad. Sci. 108 (1963), 92-105 .

[33] V.P Saxena and D. Arya, Steady state heat distribution in epidermis, dermis and sub dermal tissues, J. Theor. Biol. 89 (1981), 423-432 .

[34] V.P. Saxena, Temperature distribution in human skin and sub dermal tissues, J. Theor., Biol. 102 (1983) ,277-286 .

[35] V.P. Saxena and J.S. Bindra, Steady state temperature distribution in dermal regions of human body with variable blood flow perspiration and self controlled metabolic heat generation. Indian J. Pure Appl. Math. 15 (1) (1984), 31-42.

[36] V.P. Saxena and K.R. Pardasani, Steady State Radial Heat Flow in Skin and Underlying Tissue of Layers of Spherical regions of Human or Animal Body. Ind. J. Techn. 25 (1987), 501-505.

[37] V.P. Saxena, K.R. Pardasani, and R Agarwal, unsteady state heat flows in epidermis and dermis of human body, J. Indian Acad. Sci. (Math. Sci.), 98 (1988), 71-80.

[38] V.P Saxena and K.R Pardasani, Effect of dermal tumor on temperature distribution in skin with variable blood flow, Bull. Math. Bio. 53 (4) (1991), 525-536.

[39] N.M. Sudarshan, E.Y.K. Ng and S. L. Teh, Surface temperature distribution of a breast with and without tumor, Computer Methods Biomech. Biomed. Eng. 2(3) (1999), 187-199.

[40] M. J. de, A. Viana, F. G. de S. Santos, T. L. Rolim and R. C. F. delima. Simulating Breast Temperature Profiles through Substitute Geometries from Breast Prostheses. Proc. 17th Int. Conf. Syst. Signals Image Proc. (2010), 304-307 .

[41] https://www.healthline.com/health/breast-premenstrual-tenderness-and-swelling#outlook6

[42] http://albertathermographyclinic.com/thermograpgy/memmography